Mem. S.A.It. Suppl. Vol. , 1

Memorie della
Supplementi

Dust extinction curves of GRB host galaxies

P. Schady[1,2] T. Dwelly[3] M.J. Page[2] T. Krühler[1,4,5] J. Greiner[1] S.R. Oates[2] M. De Pasquale[2] M. Nardini[1,6] P.W.A. Roming[7] A. Rossi[8] and M. Still[9]

[1] Max-Planck Institut für Extraterrestrische Physik, Giessenbachstraße, 85748 Garching
[2] UCL Mullard Space Science Laboratory, Holmbury St Mary, Dorking, Surrey, RH5 6NT
[3] University of Southampton, Highfield, Southampton, SO17 1BJ
[4] Universe Cluster, Technische Universität München, Boltzmannstraße 2, 85748, Garching
[5] Dark Cosmology Centre, Juliane Maries Vej 30, 2100 Copenhagen
[6] University of Milano-Bicocca, IT 20126 Milano
[7] Southwest Research Institute, 6220 Culebra Rd, San Antonio, TX 78238
[8] Thüringer Landessternwarte Tautenburg, Sternwarte 5, 07778 Tautenburg
[9] NASA Ames Research Center, M/S 244-30, Moffett Field, CA 94035

Abstract. The composition and amount of interstellar dust within gamma-ray burst (GRB) host galaxies is of key importance when addressing selection effects in the GRB redshift distribution, and when studying the properties of their host galaxies. As well as the implications for GRB research, probing the dust within the high-z hosts of GRBs also contributes to our understanding of the conditions of the interstellar medium and star-formation in the distant Universe. Nevertheless, the physical properties of dust within GRB host galaxies continues to be a highly contended issue. In these proceedings we present our analysis on the mean extinction properties of dust within the host galaxies of 17 GRBs with total host galaxy visual extinction $A_V < 1$, covering a redshift range $z = 0.7 - 3.1$, and compare these results to the extinction curve properties of more heavily extinguished GRBs ($A_V > 1$).

Key words. gamma-rays: bursts – gamma-ray: observations – galaxies: ISM – dust, extinction

1. Introduction

The dust extinction along numerous lines-of-sight within the Milky Way (e.g. Savage & Mathis 1979) and the Small and Large Magellanic Clouds (SMC and LMC, respectively; Fitzpatrick 1989) have been well studied, both in terms of the absolute extinction, A_λ, at a given wavelength λ, and in terms of the relative $A_B - A_V$ extinction (i.e. the 'reddening'), $E(B-V)$. The bulk of this work has been focused on determining the relative extinction as a function of wavelength, or the *extinction law* or *curve* (e.g Cardelli et al. 1989; Gordon et al. 2003), which holds information on the grain size distribution and composition of the extinguishing dust along the observed line-of-sight. However, it has thus far only been possible to measure the dust extinction curve in extragalactic environments along lines-of-sight to bright background quasars (e.g. Maiolino et al. 2004) or gamma-ray bursts (GRBs; e.g. Watson et al. 2006; Schady et al. 2007). Long

Send offprint requests to: P. Schady

GRBs have been particularly effective at probing the extinction curve of high-z galaxies thanks to their intrinsically simple spectra (e.g. Galama & Wijers 2001; Zafar et al. 2011).

In these proceedings we discuss the variation in the dust extinction properties of star-forming galaxies using the results from a simultaneous analysis of a sample of 17 NIR to X-ray GRB afterglow SEDs. This sample has a large redshift range ($z = 0.7 - 3.1$), which provides coverage of the rest-frame wavelength dependence of extinction over several decades. As well as addressing the prominence of a Milky Way-like 2175Å feature and the presence of grey dust in GRB host galaxies, in these proceedings we also explore the uniformity of GRB host extinction laws in general.

In section 2 we give our sample selection criteria and describe our data reduction and afterglow SED analysis. Based on our individual afterglow SED analysis, we select an optimal sample of GRBs with which to study the dust extinction properties of GRB host galaxies. This final sample and the consequent simultaneous SED analysis is described in section 3. Our results are presented in section 4, and a discussion and the main conclusions from our work are provided in sections 5 and 6. Throughout the paper temporal and spectral indices, α and β, respectively, are denoted such that $F(\nu, t) \propto \nu^{-\beta} t^{-\alpha}$, and all errors are 1σ unless specified otherwise.

2. Data Sample and Reduction

2.1. Sample Selection

To study the extinction curve in the local environment of GRBs, we require a sample of bursts with afterglow data over a broad bandpass, and in particular, covering rest-frame wavelengths $\lesssim$ 2000Å, where the wavelength dependence of extinction can vary significantly between environments (e.g. SMC, LMC and Milky Way extinction curves). To carry out our analysis, we select those GRBs from the *Swift* sample up to the end of 2009 that *i*) are classified as long, *ii*) have a spectroscopic redshift, *iii*) were observed with the *Swift* X-Ray Telescope (XRT) and the UV/Optiocal Telescope (UVOT) within one hour of triggering the *Swift* Burst Alert Telescope (BAT), *iv*) had an afterglow detected by both XRT and UVOT with a peak UVOT v-band magnitude $v < 19$, and finally *v*) were detected in a total of at least four UV/optical/NIR filters, either ground based or UVOT, where at least one of these filters is at a rest-frame wavelength $\lambda < 2000$Å. A spectroscopic redshift is required in order to be able to model the intrinsic GRB afterglow spectrum, and we specify the latter three criteria in order to select GRBs that have sufficiently high quality broadband afterglow SEDs to constrain our analysis. The X-ray data provides a constraint to the afterglow intrinsic broadband spectral shape, and a further four UV-NIR datapoints are required to measure the optical spectral index, β, the flux normalisation, the total host galaxy visual, or V-band ($\lambda \sim 5500$Å) extinction, A_V, along the line-of-sight, and the UV slope of the extinction curve. This selection criteria leaves a sample of 49 GRBs out of a total of 488 GRBs observed by *Swift* by the end of 2009.

By selection, this sample of GRBs have well-sampled afterglow SEDs from which the intrinsic afterglow spectrum can be accurately modelled. However, to study the extinction curve of their host galaxies, two further selection criteria are required. Firstly, there must be evidence for host galaxy dust extinction, and secondly, the GRB afterglow should have an intrinsic power-law spectrum from the NIR through to X-ray to avoid degeneracy between the afterglow intrinsic spectral slope and the amount of dust extinction. This second level of filtering requires that we first model the SEDs of each of the initial 49 GRBs selected above.

2.2. SED analysis

We created an X-ray through to optical/NIR instantaneous SED for all 49 selected GRBs following the method described in Schady et al. (2010). The epoch of the instantaneous SED was selected to be at a time free of spectral evolution, and was chosen to minimise the interpolation in time of the optical and X-ray data.

We fitted all GRB afterglow SEDs within XSPEC (v12.5.1), first modelling the intrinsic

Table 1. Table listing our final sample of 17 GRBs with afterglows best-fit by a power-law SED model and host galaxy A_V detected at 90% confidence.

GRB	z	Host dust	A_V (mag)	$N_{H,x}$ (10^{21} cm^{-2})	β	χ^2 (dof)	Null hyp. prob.
050802	1.71	mw	0.49 ± 0.10	$2.36^{+0.75}_{-0.69}$	0.72 ± 0.04	73.4 (73)	0.466
060502A	1.51	smc	$0.59^{+0.15}_{-0.12}$	$3.62^{+1.04}_{-0.93}$	$0.76^{+0.06}_{-0.05}$	23.9 (29)	0.736
060607A	3.082	smc	0.08 ± 0.04	$12.86^{+4.09}_{-3.53}$	0.52 ± 0.02	29.3 (31)	0.555
060904B	0.703	lmc	0.15 ± 0.04	$2.98^{+0.62}_{-0.54}$	0.85 ± 0.01	36.5 (29)	0.158
060912	0.937	mw	$0.46^{+0.23}_{-0.22}$	$2.96^{+0.70}_{-0.63}$	$0.85^{+0.07}_{-0.06}$	16.0 (21)	0.770
061007	1.262	smc	0.44 ± 0.01	6.00 ± 0.21	0.89 ± 0.01	285.5 (289)	0.548
070318	0.836	smc	0.50 ± 0.04	$8.07^{+0.60}_{-0.54}$	1.14 ± 0.02	63.8 (59)	0.312
070810A	2.17	mw	$0.61^{+0.24}_{-0.21}$	$7.89^{+2.26}_{-2.02}$	$1.01^{+0.09}_{-0.08}$	18.3 (23)	0.742
071112C	0.823	smc	$0.20^{+0.05}_{-0.04}$	$0.82^{+0.89}_{-0.72}$	0.58 ± 0.02	23.7 (17)	0.128
080319B	0.937	smc	$0.06^{+0.03}_{-0.02}$	$1.13^{+0.42}_{-0.37}$	0.72 ± 0.01	15.1 (14)	0.372
080319C	1.95	smc	$0.71^{+0.08}_{-0.07}$	$8.73^{+1.12}_{-1.03}$	0.58 ± 0.04	99.7 (98)	0.432
080710	0.845	smc	0.03 ± 0.01	$0.49^{+0.29}_{-0.26}$	0.87 ± 0.01	39.2 (37)	0.370
080928	1.692	smc	0.24 ± 0.06	$3.54^{+1.14}_{-1.01}$	$1.09^{+0.04}_{-0.05}$	33.8 (30)	0.288
081008	1.968	lmc	0.29 ± 0.07	$7.60^{+1.82}_{-1.62}$	$1.13^{+0.04}_{-0.03}$	13.2 (23)	0.947
090927	1.37	mw	$0.40^{+0.18}_{-0.15}$	$2.20^{+1.52}_{-1.25}$	0.88 ± 0.08	2.2 (9)	0.989
091020	1.71	lmc	$0.86^{+0.10}_{-0.09}$	$5.12^{+0.96}_{-0.88}$	$1.09^{+0.05}_{-0.03}$	40.0 (35)	0.256
091208B	1.063	lmc	$0.95^{+0.22}_{-0.20}$	$7.81^{+1.40}_{-1.21}$	$0.90^{+0.09}_{-0.07}$	20.9 (30)	0.893

Columns (2) and (3) give the GRB redshift and the best-fit host galaxy extinction law; either smc, lmc or mw to refer to the SMC, LMC or Milky Way extinction model fit, and columns (4) to (6) are the best-fit host galaxy A_V, host galaxy N_H, and GRB energy spectral index, β. The last two columns give the χ^2 and degrees of freedom (dof), and the null hypothesis probability of the best-fit solution.

continuum with a power-law and then with a broken power-law. In the latter case the spectral break was modelled as the cooling frequency, ν_c, such that the change in slope was fixed at 0.5 (Sari et al. 1998), and the spectral break was constrained to lie within the UV to X-ray energy range. We considered a broken power-law model to provide a better fit to the afterglow spectral continuum when the F-test returned a null hypothesis probability smaller than 5%.

The XSPEC model components *phabs* and *zphabs* were used, respectively, to fit the Milky Way and host galaxy photoelectric absorption, and *zdust* was used to model dust extinction in the Milky Way and host galaxy. We assumed solar metallicity abundances, both in the case of the Milky Way and GRB host galaxy, and we used the XSPEC default solar abundances (Anders & Grevesse 1989). We fixed the Galactic reddening, $E(B-V)_{Gal}$, and the Galactic neutral hydrogen column density $N_{H,Gal}$, to the values from the Galactic maps of Schlegel et al. (1998) and Kalberla et al. (2005), respectively. The Galactic dust extinction was modelled on the mean Milky Way extinction law as parameterised by Pei (1992), which has the total-to-selective extinction, $R_V = A_V/E(B-V)$ set to the average value of 3.08 measured in the Milky Way diffuse ISM.

We modelled the dust extinction within the GRB host galaxy on the mean SMC, LMC and Milky Way extinction curves (Pei 1992), which become increasingly flatter blueward of $\sim$ 2500Å, and have an increasingly pronounced broad extinction feature centred at $\sim$2175Å (see Fig. 1). These three curves thus provide good coverage of the range in extinction curves observed in the local Universe. To remain consistent with Pei (1992), we fixed the total-to-selective extinction of the mean SMC, LMC and Milky Way extinction curves to $R_V =$ 2.93, 3.16 and 3.08, respectively. This left only

the total host galaxy dust reddening along the line-of-sight, $E(B-V)$, free to vary.

3. The GRB mean extinction curve

To study the dust extinction curve within GRB host galaxies, we wish first to reduce our sample of 49 GRBs down to those that have both a significant host galaxy dust extinction signature imprinted on their SED and that have a single power-law NIR to X-ray spectral component. This latter requirement is applied because of the degeneracy between the best-fit optical spectral index and the steepness of the extinction curve fitted to the SED. Of the 49 GRBs analysed, 25 did not require a spectral break between the X-ray and optical wavelength ranges. As a consistency check on our SED analysis, we also verified that the temporal decay slope in the X-ray and optical bands was the same within 1σ errors at the epoch of the instantaneous SED. 36 of the 49 GRBs had a host galaxy A_V measured to be greater than zero at the 90% confidence, and 17 of these were best-fit by a single spectral component, and thus made our final sample. In Table 1 we summarise the best-fit model results for each of the 17 GRBs in our prime sample.

To investigate the mean shape of the extinction curve in the host galaxies of our sample of 17 GRBs, we applied a simultaneous fit to all 17 NIR to X-ray broadband SEDs using similar models as those described in section 2.2. However, in addition to the SMC, LMC and Milky Way extinction laws previously fitted to the afterglow SEDs, we also fitted the more general extinction curve model developed by Fitzpatrick & Massa (1990) to our data, which we shall refer to as the FM90 model. This latter extinction curve model has eight free parameters that are able to fit variations in the NIR and UV curvature and in the prominence of the 2175Å feature observed along lines-of-sight within local and extragalactic galaxies. The large number of degrees of freedom in the FM90 model did not make it a feasible model to use in the individual afterglow SED analysis. However, the large number of data points in our simultaneous fit provide sufficient constraint for the FM90 model to be fitted to the data. Additionally, the widespread use of this model allows us to compare our best-fit results to the dust extinction properties of other local and extragalactic environments.

The eight free parameters of the FM90 model are made up of the total galaxy dust reddening, $E(B-V)$, the total-to-selective dust extinction, R_V, and six further coefficients. These six coefficients define the linear extinction component underlying the UV range (c_1 and c_2), the height (c_3), width (γ), and central wavelength (x_c) of the 2175Å bump, which is modelled with a Lorentzian-like *Drude* profile ($D(x;\gamma,x_c)$), and the far-UV curvature (c_4). The UV intercept, c_1, and the UV slope, c_2, are tightly correlated, with the most recent analysis showing a linear dependence of $c_1 = 2.09 - 2.89c_2$ (Fitzpatrick & Massa 2007). Furthermore, the central wavelength of the 2175Å bump does not vary significantly. We therefore fix x_c to the mean observed value of 4.592 μm^{-1}, and tie c_1 to c_2, as described above, leaving us with six free parameters. Given the typically weak signature of a bump in the extinction law of GRB host galaxies together with the low spectral resolution available from our broadband data, the constraint on the remaining two bump parameters (i.e. c_3 and γ) is small, and we therefore also fixed the width of the bump, γ, to the median Milky Way value of $\gamma = 0.922$ (Fitzpatrick & Massa 2007). This allows for a more realistic measurement of the bump strength or an upper limit, provided by the parameter c_3.

In its original form the FM90 model is only valid up to wavelengths $\lambda < 2700$Å (rest-frame). Furthermore, most of the GRBs in our sample do not have sufficient data at rest-frame NIR wavelengths to derive the total-to-selective extinction, which is given by $R_V = 1.10E(V-K)/E(B-V)$ (Morgan & Nandy 1982). We therefore appended the mean LMC extinction curve to the FM90 analytic model to cover the extinction at wavelengths $\lambda > 2700$Å, and fixed R_V to the mean LMC value, R_V=3.16 (Pei 1992). We chose the LMC curve because it has a continuum that is mid-way between that observed in the SMC and Milky Way. Nevertheless, all well-observed extinction curves in the local Universe are com-

Table 2. Best-fit results from our simultaneous SED analysis.

Model	c_1 $= 2.09 - 2.84c_2$	c_2	c_3	c_4	$\chi 2/dof$	Null hyp. prob.
FM90						
All data	-2.66	$1.67^{+0.81}_{-1.51}$	$0.00^{+0.67}_{-0.00}$	$0.43^{+0.14}_{-0.11}$	819.9/846	0.734
$\lambda_{UV} > 121nm$	-1.64	$1.31^{+0.79}_{-1.20}$	$0.14^{+0.57}_{-0.18}$	$1.80^{+1.29}_{-0.64}$	813.8/814	0.495
SMC						
All data	*-4.47±0.19*	*2.35±0.18*	*0.08±0.01*	*-0.22±0.01*	815.0/812	0.464
$\lambda_{UV} > 121nm$					786.5/781	0.438
LMC						
All data	*-2.16±0.36*	*1.31±0.08*	*1.92±0.23*	*0.42±0.08*	818.7/812	0.428
$\lambda_{UV} > 121nm$					795.4/781	0.352
Milky Way						
All data	*0.12±0.11*	*0.63±0.04*	*3.26±0.11*	*0.41±0.02*	1333.1/812	$5.5e^{-28}$
$\lambda_{UV} > 121nm$					1276.3/781	$1.7e^{-26}$

NOTE- Table lists results from both the analysis that used all available afterglow SED data, and from the analysis where data covering the Lyman-forest were excluded (i.e. no UV data at wavelengths $\lambda <$ 121.5 nm) . The best-fit Fitzpatrick & Massa (1990) (FM90) parameterisations to the SMC, LMC and Milky Way models from Clayton et al. (2003) are shown in italic as a comparison to the best-fit FM90 fits to our data.

parable redward of 2500Å, and the specific choice of these appended to the Fitzpatrick & Massa (1990) model at $\lambda > 2700$Å has only a marginal effect on our results.

In our simultaneous SED analysis, all dust extinction models fitted had the strength of the host galaxy reddening, E(B-V), as a free parameter for each GRB, but all other dust parameters were tied between GRBs. The spectral index of the continuum, β, and the amount of host metal absorption, N_H, were also left free to vary for each GRB.

4. Results

The simultaneous best-fit extinction curves fitted to our data are plotted in Fig. 1, all normalised at $\lambda = 3000$Å. The shaded grey area is the 90% confidence region to the best-fit FM90 model. A summary of our best-fit results is given in Table 2, and to place our best-fit FM90 coefficients in context, in this table we also list the FM90 best-fit coefficients to the average SMC, LMC and Milky Way extinction laws (Clayton et al. 2003, and references therein).

We find that the Milky Way mean extinction law cannot adequately fit the host galaxy extinction properties of our sample of GRB afterglows, and is rejected at 99.99% confidence (see Table 2). This is also illustrated by the inconsistency between the best-fit FM90 extinction curve and the Milky Way mean extinction curve plotted in Fig. 1, where the latter is significantly flatter and has a more pronounced 2175Å bump. Both the SMC and LMC mean extinction laws, on the other hand, provide good fits to the data. The best-fit FM90 UV continuum is in closer agreement to the LMC rather than the SMC UV extinction slope, although at the location of the 2175Å bump, the best-fit FM90 model is closer to the featureless SMC curve. Nevetherless, the 90% confidence region of the FM90 model plotted in Fig. 1 shows that the presence of a weak 2175Å bump cannot be ruled out by our data.

We used the best-fit FM90 extinction curve from our simultaneous SED analysis to re-fit the SEDs of all 49 GRBs that were in our initial sample. In these fits, all FM90 parameters were fixed to their best-fit value from our simultaneous analysis, and only the host galaxy reddening, $E(B-V)$, was left free to vary. This host extinction curve model provided an acceptable fit to all 49 GRB afterglow SEDs, and compared to the SMC, LMC and Milky Way

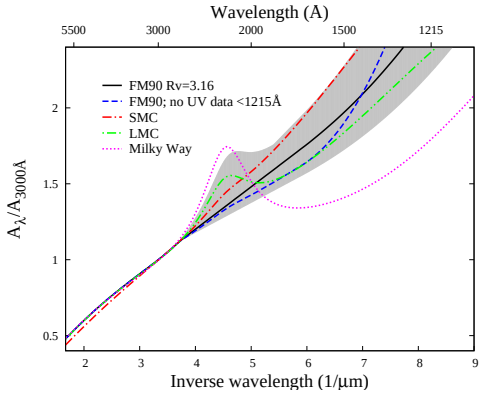

Fig. 1. Best-fit mean GRB host extinction law as derived from our simultaneous SED fits normalised at $A_{3000Å}$ and corresponding 90% confidence region (grey). The best-fit FM90 model is plotted in black (solid), and the best-fit model to the SEDs with UV data blueward of 1215Å omitted is shown in blue (long-dashed). Also shown for comparison are the mean SMC (red, dot-dash), LMC (green, dot-dot-dash) and Milky Way (pink, dotted) extinction laws, using the parameterisation from (Pei 1992).

models, improved the fit for 65-70% of the GRBs with host galaxy dust extinction measured at 90% confidence. For the remaining 30-35%, the goodness of fit worsened by a median of $\langle\Delta\chi^2\rangle = 1$ relative to the SMC fit, but by $\langle\Delta\chi^2\rangle = 5$ for the Milky Way fit. By allowing the height of the 2175Å bump to vary, the fraction of GRBs better fit by the FM90 model rose to $\sim$ 80%. This indicates that for at least 10–15% of the extinguished GRBs in our sample, the host galaxy extinction curve has a 2175Å feature. This is in good agreement with the results from Zafar et al. (2011), who studied the extinction curve for a sample of 41 GRB afterglows using combined, broadband photometric and spectroscopic data. In their analysis, they found $\sim$ 85% of their extinguished sample to be best-fit by SMC-type extinction, and $\sim$ 10% to be best-fit by an extinction curve model with a 2175Å feature.

5. Discussion

In our analysis on the host galaxy dust extinction imprinted on the UV through to NIR afterglows of a prime sample of 17 GRBs, we find the best-fit model to be consistent with both the mean SMC and LMC extinction curve. This is in agreement with the results from several previous studies on the dust extinction properties of GRB hosts (e.g. Stratta et al. 2004; Kann et al. 2006; Starling et al. 2007; Schady et al. 2007, 2010; Greiner et al. 2011). Nevertheless, the shape of our best-fit GRB host extinction curve strongly contrast with the extinction curves of the highly extinguished GRBs 070802 and 080607 measured in Elíasdóttir et al. (2009) and Perley et al. (2011) respectively, and GRB 080605 and GRB 080805 as measured by Zafar et al. (2011), all of which are flatter and have a clear 2175Å feature. None of these GRBs were included in our sample due to the faintness of their observed optical afterglows. The possible systematic uncertainties present in our analysis, as well as the selection effects in our sample and discussed in greater detail in our paper (Schady et al. 2012). In these proceedings we focus on the properties of those GRBs in our sample relative to those of GRBs with distinct host dust extinction properties.

5.1. A_V dependent extinction curves

By requiring that the GRBs in our sample have both a spectroscopic redshift measurement and a UVOT v-band magnitude $v < 19$ we remove GRBs from our sample with highly extinguished afterglows, both due to dusty regions within their host galaxy and/or high Galactic extinction along their line-of-sight. If the extinction law of GRB host galaxies varies with the host galaxy dust column density, then our analysis will clearly only be applicable to GRBs with a host galaxy visual extinction smaller than a certain threshold, above which the GRB afterglow would be too extinguished to enter our sample. There is empirical evidence that the prominence of the 2175Å extinction bump is related to the total visual extinction, A_V, along the line-of-sight. The host extinction curves of GRB 070802, GRB 080605, GRB 080607 and GRB 080805 are the only ones with a spectroscopically detected 2175Å extinction bump, and the af-

terglows are also of the most heavily extinguished.

Such a relation between the prominence of the 2175Å feature and visual extinction, A_V, is not necessarily indicative of evolution in the dust extinction curve, and may be a result of there not being sufficient extinction in low dust environments for the 2175Å feature to be detected with any statistical significance. It is, nevertheless, possible that the results presented here are only valid for the host galaxies of those GRBs that have a total visual extinction $A_V < 1$. In view of this prospect, in the next section we investigate further the origin of differences in the host galaxy extinction curves of GRBs with only moderately extinguished afterglows, such as in our sample, and those that are highly extinguished (i.e. $A_V > 1$).

5.2. Variation in host extinction curves

The improved positional accuracy of GRBs provided by the rapid response of *Swift* and (semi-)robotic ground-based telecopes, in particular those equipped with NIR instruments, has significantly improved our capabilities over the last half decade to study highly dust-extinguished GRBs and their host galaxies. Dedicated host galaxy follow-up programmes of highly dust-extinguished GRB candidates are revealing a sample of GRB host galaxies that are typically more massive, luminous, and chemically evolved than the typical host galaxies of relatively unextinguished GRBs (GRB 020127; Berger et al. 2007, GRB 030115; Levan et al. 2006, GRB 070802; Krühler et al. 2011, GRB 080325; Hashimoto et al. 2010, GRB 080607; Chen et al. 2011).

In the case of GRB 080607, Prochaska et al. (2009) argued the majority of the afterglow dust extinction to come from dust within an intervening molecular cloud. However, it is notable that the characteristic properties of the host galaxy are also atypical when compared to optically-selected samples (Chen et al. 2011). The host galaxy of GRB 080607 had a stellar mass $M_* \sim 8 \times 10^9\ M_\odot$, which is almost an order of magnitude larger than the mean stellar mass of optically selected samples ($\langle M_* \rangle \sim 10^9\ M_\odot$; Savaglio et al. 2009; Krühler et al. 2011), and it was very red, with $R - K > 5$ (Chen et al. 2011). This is also the only GRB to have a robust detection of molecular hydrogen absorption in its afterglow spectrum (Prochaska et al. 2009).

On the other hand, GRB 070306 and GRB 100621A were heavily extinguished GRBs ($A_V \sim 5.5$ and $A_V \sim 3.8$ respectively), but both had very blue host galaxies, with $R-K$ colours comparable to the host galaxies of relatively unextinguished GRBs (e.g Krühler et al. 2011), indicative of a very clumpy distribution of dust. Furthermore, although GRB 070306 had one of the largest stellar masses measured for a long GRB host galaxy ($2 \times 10^{10}\ M_\odot$; Krühler et al. 2011), the host stellar mass for GRB 100621 ($10^9\ M_\odot$) was comparable to that of optically bright afterglow host galaxies. The relation between afterglow dust extinction and host galaxy properties, including the host extinction curve, is therefore not clear, and further investigation of the host galaxies of heavily extinguished afterglows will be needed to address these issues.

6. Conclusions

Using a sample of 17 GRBs with good wavelength coverage and a single NIR through to X-ray spectral emission component, we have been able to constrain the host galaxy dust extinction properties as a function of wavelength for GRBs with total host galaxy visual extinction $A_V < 1$. By studying the host galaxy dust extinction properties for a sample of GRBs rather than for a single, well-observed, case, we have been able to investigate the average dust extinction properties in the host galaxies of GRBs, albeit only for those with a moderate host galaxy visual extinction ($A_V < 1.0$). Using the Fitzpatrick & Massa (1990) analytic extinction curve model to fit our afterglow sample, we find the best-fit to have a slope blueward of $\sim$ 2000Å that is intermediate to that of the SMC and LMC mean extinction curves, and it has no 2175Å extinction bump. Within the uncertainties, the best-fit extinction law is consistent with both the SMC and LMC mean extinction curves. However, our data are inconsistent with having a host galaxy extinction curve as

flat as the average Milky Way curve blueward of ~ 2000Å.

Our best-fit FM90 parameterisation of the GRB host extinction curve provides an acceptable fit (at 3σ confidence) to a full sample of 49 afterglow SEDs that we initially analysed, providing typically a similar or improved fit to the afterglow SEDs compared to fits that use local dust extinction curve models. Of those GRBs with host galaxy dust extinction measured at 90% confidence, around 10% were, however, better fit by an extinction curve that contained the 2175Å dust feature. Furthermore, up to 12% of the 49 afterglow SEDs analysed could have a host galaxy extinction curve that is significantly flatter at rest-frame UV wavelengths than the mean Milky Way extinction curve. For this 12% of GRBs, the improved fit provided by a flatter UV-extinction curve model increases the host galaxy total extinction relative to fits with local extinction curve models. This is compatible with the trend increasingly observed between significantly extinguished GRBs ($A_v \gg 1$) and flat host galaxy extinction curves.

The relatively UV-steep host galaxy extinction curve for our sample of modestly extinguished GRBs, and the much flatter extinction curves with more pronounced 2175Å features of host galaxies of more extinguished GRBs, is adding to the empirical evidence that the extinction curve of GRB hosts vary as a function of host dust abundance and/or some other galaxy property.

Acknowledgements. This research has made use of data obtained from the High Energy Astrophysics Science Archive Research Center (HEASARC), the UK Swift Science Data Centre at the University of Leicester and the Leicester Data base and Archive Service (LEDAS), provided by NASAs Goddard Space Flight Center and the Department of Physics and Astronomy, Leicester University, UK, respectively.

References

Anders, E., & Grevesse, N. 1989, GeCoA, 53, 197
Cardelli, J. A., Clayton, G. C., & Mathis, J. S. 1989, ApJ, 345, 245
Chen, H.-W., et al. 2011, ApJ, 727, L53
Clayton, G. C., et al. 2003, ApJ, 588, 871
Elíasdóttir, Á., et al. 2009, ApJ, 697, 1725
Fitzpatrick, E. 1989, Interstellar Dust, 135, 37
Fitzpatrick, E. L., & Massa, D. 1990, ApJS, 72, 163
Fitzpatrick, E. L., & Massa, D. 2007, ApJ, 663, 320
Galama, T. J., & Wijers, R. A. M. J. 2001, ApJ, 549, L209
Gordon, K. D., et al. 2003, ApJ, 594, 279
Greiner, J., et al. 2011, A& A, 526, A30
Kalberla, P. M. W., et al. 2005, A& A, 440, 775
Kann, D. A., Klose, S., & Zeh, A. 2006, ApJ, 641, 993
Krühler, T., et al. 2011, A& A, submitted
Maiolino, R., et al. 2004, Nature, 431, 533
Morgan, D. H., & Nandy, K. 1982, MNRAS, 199, 979
Pei, Y. C. 1992, ApJ, 395, 130
Perley, D. A., et al. 2011, AJ, 141, 36
Prochaska, J. X., et al. 2009, ApJ, 691, L27
Sari, R., Piran, T., & Narayan, R. 1998, ApJ, 497, L17
Savage, B. D., & Mathis, J. S. 1979, Annu. Rev. Astron. Astrphys., 17, 73
Savaglio, S., Glazebrook, K., & Le Borgne, D. 2009, ApJ, 691, 182
Schady, P., et al. 2007, MNRAS, 377, 273
Schady, P., et al. 2010, MNRAS, 401, 2773
Schady, P., et al. 2012, A&A, submitted
Schlegel, D. J., Finkbeiner, D. P., & Davis, M. 1998, ApJ, 500, 525
Starling, R. L. C., et al. 2007, ApJ, 661, 787
Stratta, G., et al. 2004, ApJ, 608, 846
Watson, D., et al. 2006, ApJ, 652, 1011
Zafar, T., et al. 2011, A&A, 532, A143